24/phdac/04 Majeed Abdulameer Shaheed Alarjaw...

Novel Tannin and Cassia fistula gum crosslinked hydrogel for Controlled Release of Thiamethoxam

Plag check

Document Details

Submission ID
trn:oid:::27535:144208270

Submission Date
Jun 25, 2026, 1:23 PM GMT+3

Download Date
Jun 25, 2026, 1:33 PM GMT+3

File Name
Novel Tannin and Cassia fistula gum crosslinked hydrogel for Controlled Release of Thiametho....docx

File Size
6.9 MB

37 Pages

5,459 Words

33,356 Characters

8% Overall Similarity

The combined total of all matches, including overlapping sources, for each database.

Filtered from the Report

- Bibliography
- Quoted Text
- Small Matches (less than 8 words)

Exclusions

- 23 Excluded Matches

Match Groups

56 Not Cited or Quoted 8%
Matches with neither in-text citation nor quotation marks

0 Missing Quotations 0%
Matches that are still very similar to source material

0 Missing Citation 0%
Matches that have quotation marks, but no in-text citation

0 Cited and Quoted 0%
Matches with in-text citation present, but no quotation marks

Top Sources

6% Internet sources
1% Publications
2% Submitted works (Student Papers)

Match Groups

- **56** Not Cited or Quoted 8%
  Matches with neither in-text citation nor quotation marks
- **0** Missing Quotations 0%
  Matches that are still very similar to source material
- **0** Missing Citation 0%
  Matches that have quotation marks, but no in-text citation
- **0** Cited and Quoted 0%
  Matches with in-text citation present, but no quotation marks

Top Sources

6% Internet sources
1% Publications
2% Submitted works (Student Papers)

Top Sources

The sources with the highest number of matches within the submission. Overlapping sources will not be displayed.

1	Internet	nopr.niscpr.res.in 5%
2	Publication	Enas M. Ahmed. "Hydrogel: Preparation, characterization, and applications: A revi... <1%
3	Internet	saarj.com <1%
4	Student papers	Lehigh University on 2014-04-30 <1%
5	Internet	ics.utsa.edu <1%
6	Internet	journal.ugm.ac.id <1%
7	Student papers	Higher Education Commission Pakistan on 2011-08-07 <1%
8	Publication	Mohamed El Farkhani, Omar Azougagh, Said Dadou, Soufian El Barkany, Mohame... <1%
9	Student papers	61459 on 2015-06-11 <1%
10	Student papers	Universiti Malaysia Pahang on 2022-01-15 <1%

11 Student papers

University of New South Wales on 2010-04-28 <1%

12 Internet

baadalsg.inflibnet.ac.in <1%

13 Publication

de Oliveira Henriques, Marta Alexandra. "Poly(Ionic Liquid) Derived Materials for ... <1%

14 Publication

Biomedical Applications of Hydrogels Handbook, 2010. <1%

15 Student papers

Heriot-Watt University on 2012-08-14 <1%

16 Publication

Johnson, Leah C.. "Synthesis and Characterization of Poly(γ-Benzyl-L-Glutamate) b... <1%

17 Publication

Masrat Maswal, Oyais Ahmad Chat, Aijaz Ahmad Dar. "Rheological characterizati... <1%

18 Publication

Meenakshi Tanwar, Rajinder K. Gupta, Archna Rani. "Natural gums and their deri... <1%

19 Student papers

University of Leicester on 2007-08-14 <1%

20 Internet

doczz.net <1%

21 Internet

www.mdpi.com <1%

ABSTRACT

Pesticide residues in soil and runoff water pose threats to both humans and the environment, necessitating innovative solutions. As controlled-release matrices, hydrogels offer a promising approach to mitigate this issue. Natural polymer-based hydrogels are widely synthesised due to their significant impact on the physicochemical and mechanical properties. Being naturally abundant, *Cassia fistula* (CF) and Tannin from *Acacia catechu* (ACT) could be potentially used to produce CFAC-*g*-SAH for effective controlled-release hydrogels for agrochemicals. The synthesised hydrogels were thoroughly characterised by FT-IR, ^{13}C NMR, SEM, TGA, and XRD to observe structural, morphological, and thermal changes. CFAC-*g*-SAH was compared with ACT and CF hydrogels. The swelling studies of the synthesised hydrogel were measured by varying amounts of crosslinker and biopolymer, yielding the highest swelling for CFAC-*g*-SAH of 185.94 $g \cdot g^{-1}$. The loading percentages of thiamethoxam were 58.49%, 36.39%, and 42.43% for CFAC-*g*-SAH, CF-*g*-SAH, and ACT-*g*-SAH, respectively. The CFAC-*g*-SAH hydrogel outperformed ACT-g-SAH and CF-g-SAH in highest swelling and longest release duration. A sustained release of up to 40 hours was achieved using CFAC-*g*-SAH hydrogel, followed by a non-Fickian release mechanism. Thus, the synthesised CFAC-*g*-SAH hydrogel emerges as a promising controlled-release device for agrochemicals with the potential to mitigate the environmental impact of pesticide residues.

TABLE OF CONTENTS

LIST OF FIGURES AND SCHEMES

LIST OF TABLES

ABBREVIATIONS

ACT	*Acacia Catechu* (Tannin)
CF	*Cassia fistula*
KPS	Potassium per sulphate
MBA	N, N′-Methylenebisacrylamide
AA	Acrylic Acid
SAH	Super Absorbent Hydrogel
KP-MODEL	Korsmeyer-Peppas model
SEM	Scanning Electron Microscopy
XRD	X-ray Diffraction
FT-IR	Fourier-transform infrared spectroscopy
NMR	Nuclear Magnetic Resonance
TGA	Thermogravimetric Analysis

CHAPTER 1: INTRODUCTION

Agricultural production is highly dependent on the use of pesticides and water availability for irrigation. Pesticides prevent crops from insects, weeds, fungi and other harmful pests. In traditional methods, pesticides are applied to the entire crop, resulting in significant losses from leaching. They may reduce the efficacy of the pesticide or harm non-target organisms. The overuse and depletion of water resources threaten the livelihoods of agriculture and water-dependent communities. Furthermore, globally, agricultural output would have to increase by 50% and water use by 15% by 2050 to feed a population of almost 9 billion people [1]. A natural polymer-based hydrogel can be used as a controlled-release device to address this problem. Controlled release of pesticide is a type of chemical method in which a synthesised hydrogel delivers the pesticide effectively to the designated area for a prolonged period of time, with a slower rate [2]. This technique prevents excessive water use, enhances soil quality, and prevents pesticide leaching. Hydrogels absorb water, expand, and gradually release the encapsulated active ingredient via a controlled active agent diffusion mechanism. It acts as a treatment to mitigate the adverse effects of direct pesticide application. By using controlled release technologies with functional polymers, hydrogels reduce soil contamination, water eutrophication, pesticide leaching, and water pollution while increasing pesticide efficiency. Natural biopolymers are one of the efficient choices for hydrogel formation due to their biocompatibility and biodegradability [3].

Natural gums, as polysaccharides, are mainly composed of sugars, and they provide enhancement in the viscosity of the solution. Natural gums contain numerous hydrophilic components that can form interactions, such as hydrogen bonding, which play a significant role in the synthesis of hydrogel. Since natural gums are cost-effective and non-toxic materials, they are widely used in the process of forming hydrogel for agricultural, industrial and biomedical applications [4]. Natural gums are classified by source. Mostly, plant-based gums are found inside the seed or the wood/bark part of the plant. For example, guar gum, locust bean gum and *Cassia fistula*, etc., are found in the seed of the plant. To be more specific, gums are mainly obtained from the endosperm of some seeds [5]. *Cassia fistula* (CF) is a neutral polysaccharide seed gum isolated from the endosperms of the plant. The parent chain of this gum is made up

of a linear chain of mannose residues with 1,4-linkage, with small lateral branches made up of 1,6-linked galactose residues, as shown in Figure 1(a) [6]. Many metabolites found in *Cassia* species can have specific physiological effects on the bodies of humans, animals, or plants [7].

Polyphenols are one of the types of natural polymers obtained from plants, mainly in plant tissues. Polyphenolic compounds contain a large number of phenolic groups that can be attached to simple aromatic structures or to complex compounds such as tannins, depending on their composition [6]. Tannins are polyphenols, found in plants. Tannins are classified into two categories based on their structural characteristics and properties as hydrolysed and condensed tannins. Condensed tannins are flavonoids that contain catechin and epicatechin. Tannin from *Acacia catechu* (ACT) is a deciduous tree belonging to the Fabaceae family. It is also known as *Senegalia* catechu and is widely distributed across South and Southeast Asia. Its heartwood extract, sometimes known as catechu or katha, contains antioxidant properties. Catechu is rich in tannin, which contains polyphenolic groups, due to which it can also be used as a crosslinker [8], [9]. Due to the presence of a large number of aromatic rings and hydroxyl groups, polyphenols can interact with various substances via electrostatic interactions and hydrogen bonding. Also, it can enhance the stability and bioavailability of the compound [10]. Pesticides are an essential component in the agricultural sector and global food supply, as they protect crops from pests and weeds [11]. However, due to factors like wind dispersal and air pressure variations, the application of pesticides in an open system is ineffective, and there's potential loss of pesticides [12]. Hydrogel can encapsulate pesticides inside its matrix and release them slowly; this slow release maintains an effective concentration of pesticides in the soil without any wastage of pesticide [13]. This controlled-release system works by encapsulating the pesticide in a hydrogel (ex-situ encapsulation) and allowing it to diffuse out of the hydrogel as it absorbs water from the soil. This mechanism generally proceeds via a 1st-order reaction. This slow release of pesticides accelerates plant growth in a better way [14]. The class of neonicotinoids used as insecticides contain thiamethoxam, which is a white crystalline, odourless compound. It is a 2nd generation neonicotinoid. They interact with the nicotinic acetylcholine receptor protein found in insect nerve fibre membranes [15]. Pesticide used for controlled release is Thiamethoxam (Figure(1b)). IUPAC nomenclature of thiamethoxam (3-

(2-chloro-1,3-thiazol-5-methyl-1,3,5-oxadiazinan-4-ylidene(nitro)amine).

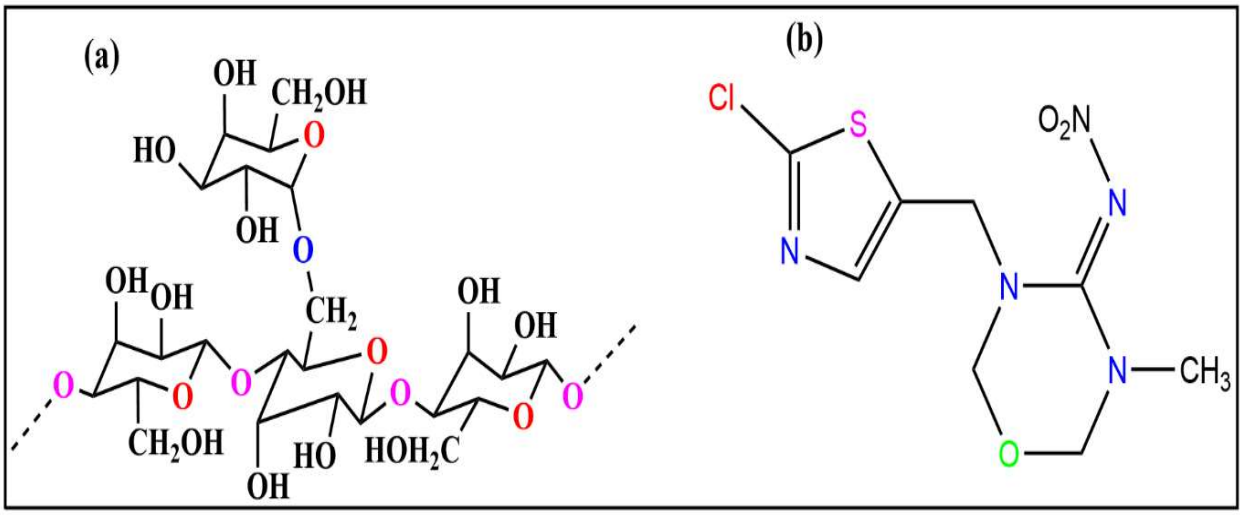

Figure 1 Structure of (a) *Casia fistula* and (b) Thiamethoxam

This work focuses on the fabrication of hydrogels from *Cassia fistula* and Tannin from *Acacia catechu* by varying the amount of biopolymer and crosslinker. These biopolymers are crosslinked with the crosslinker N,N′-Methylenebisacrylamide (MBA). A total of 16 formulations were synthesised for optimisation, and control hydrogels ACT-g-SAH and CF-g-SAH were also synthesised for comparative studies. A swelling study of CFAC-g-SAH, CF-g-SAH and ACT-g-SAH was studied for approximately 50 hours. The highest swelling Index was obtained for CFAC-g-SAH6. Synthesised hydrogels were characterised for structural and morphological analysis. For functional group determination and structural analysis, ^{13}C NMR and FT-IR spectroscopic techniques were used. For surface morphology, PXRD and SEM analyses were performed. The release kinetics of thiamethoxam in distilled water were studied to assess the potential of the developed hydrogel as an eco-friendly pesticide delivery system.

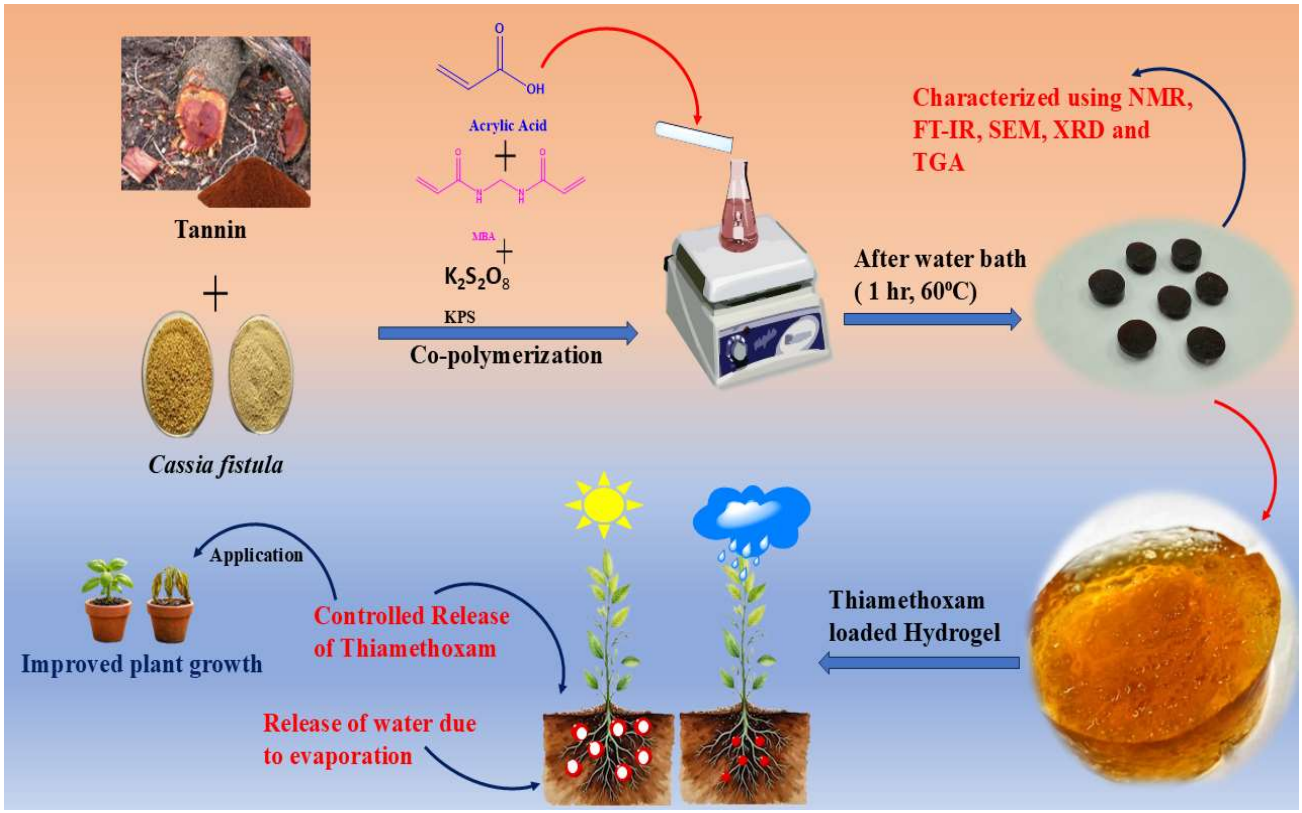

GRAPHICAL ABSTRACT

CHAPTER 2: LITERATURE REVIEW

2.1 Hydrogels

Hydrogels are 3D networks synthesised from natural polymers or gums via chemical or physical crosslinking techniques. They have a strong tendency to absorb water due to their hydrophilic nature. In chemical method, crosslinking hydrogels are formed by mainly by free radical polymerisation and Schiff base reaction. Adding a crosslinker between polymer chains changes the polymer's physical characteristics depending on the degree of crosslinking as well as whether crystallinity is present or not. A chemically crosslinked hydrogel is often strong and permanent due to chemical bonding. Also, they have strong mechanical strength, whereas a physically crosslinked hydrogel is formed by non-covalent bonding like Vanderwall interaction, hydrogen bonding, ionic bonding, etc [16]. Hydrogels can swell up an exceptionally large amount of water and maintain their matrix. Hydrogels have high porosity and, after absorbing water, become soft and fragile. Due to these properties, they show resemblance to tissues [17], [18]. A chemically crosslinked hydrogel is often strong and permanent due to chemical bonding, which provides it with mechanical strength [5]. Hydrogels can be synthesised from natural polymers or synthetic polymers. Hydrogel synthesised from natural polymers like polysaccharides shows good biocompatibility and biodegradability. Cellulose, chitosan, alginate, etc., and their derivatives can be used for making hydrogels. These are ideal for the fabrication of hydrogel due to the different functional groups present in them, such as hydroxyl group, carboxyl group, amino group, etc. Hydrogels synthesised from natural polymers, such as polysaccharides, exhibit biocompatibility and biodegradability. These are ideal for the fabrication of hydrogel due to the different functional groups present in them, such as hydroxyl group, carboxyl group, amino group, etc [19]. Hydrophilic functional groups on polymer backbone give hydrogels the capacity to absorb water, while cross-links between the network chains confer resistance to dissolution. The most important characteristic of natural polymer-based hydrogels is that they are non-toxic, eco-friendly and biodegradable. Hydrogels have many applications in agriculture, the food industry, the cosmetic industry, and the pharmaceutical industry [20].

2.2 Classification of Hydrogels

Hydrogels are classified based on their physical properties, type of swelling, origin, ionic charge, sources, biodegradation rate, and detected crosslinking. In general, either synthetic or biological components can be used to create hydrogels. Petroleum-based ingredients are found in synthetic polymers, whereas natural materials, including cellulose, starch, lignin, and kenaf fibre, are found in bio-based hydrogels. Compared to hydrogels made from biological materials, synthetic hydrogels are less hydrophilic and more resilient mechanically [21].

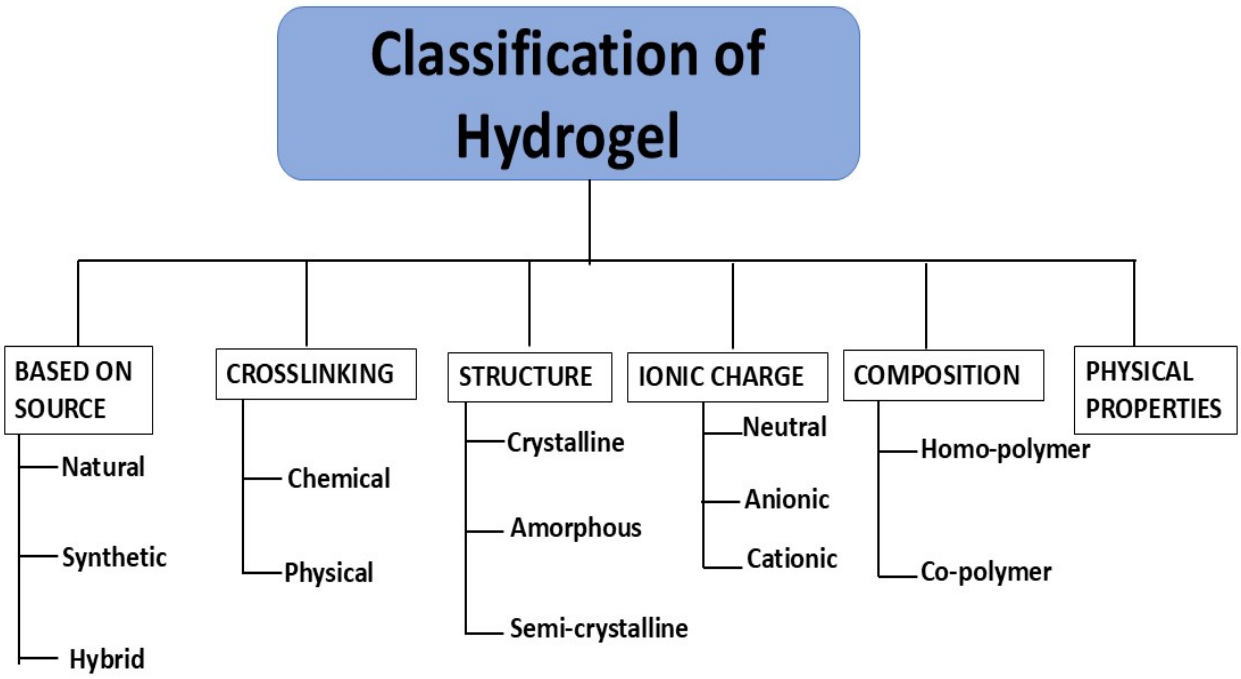

2.2.1 Based on sources

Depending upon the sources, hydrogels are divided into three categories: Synthetic, Natural, and Hybrid. Polyacrylamide, polyvinyl alcohol, and polyethene oxide are examples of synthetic hydrogels that were first used in agricultural settings. Nevertheless, it was later found that these hydrogels might be environmentally dangerous [22]. Synthetic hydrogels have a moderate degradation rate, a high degree of swelling, and a high degree of resilience. On the other hand, hydrogels derived from natural polymers exhibit minimal swelling and a weak structure. Ahmadi et al. claim that hydrogels derived from natural polymers are biodegradable. Some examples of natural gums are guar gum, *Cassia fistula*, xanthan gum, etc. On rare occasions, the breakdown products may even increase the soil's

fertility. The advantages of both natural polymer-based hydrogel and synthetic hydrogel can be combined by crosslinking natural polymers onto synthetic polymers to create a new class of hydrogels.

2.2.2 Based on Crosslinking

The polymers' capacity to create elastic three-dimensional matrices that allow swelling while preserving the matrix's structure is entirely due to crosslinking. Ionic interactions, hydrogen bonds, hydrophobic interactions, graft polymerisation, network creation of a water-soluble polymer, and crosslinking can all be used to chemically and physically crosslink hydrogels [23]. Chemically and physically crosslinked hydrogels differ in that the former have temporary bonds, whereas the latter have long-term ones. The hydrogel's strength and durability come from chemical crosslinking, which is irreversible. Applications involving high temperatures, fluctuating pH levels, and pressure can benefit from this capability. Because physical cross-linking reacts quickly to destabilisation in response to external stimuli, it is reversible.

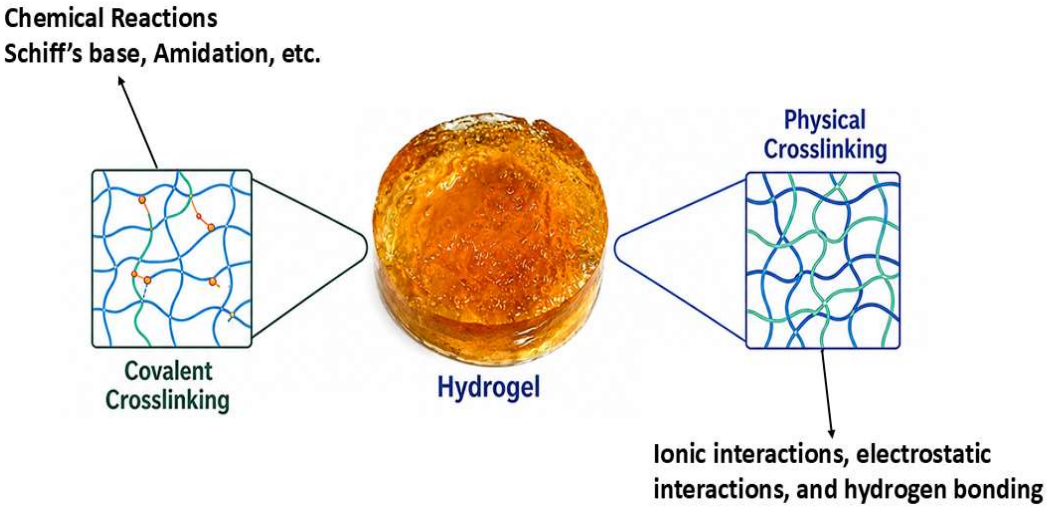

2.2.3 Based on Composition

(a) Homopolymer: Made of a single species of monomer, which is the key structural ingredient of all polymer networks, these are known as polymer networks. The skeleton of homopolymers may be cross-linked, depending on the kind of monomer and the polymerisation process.

(b) Co-polymer: These are constituted of two or more different monomer species with at least one hydrophilic component, organised in a random, block or alternating configuration in the polymeric network.

2.3 Application of Natural Gum-based Hydrogels

Hydrogels derived from Natural gum are non-toxic and safe; due to this, it has wide applications in different industries such as agriculture, drug delivery, biosensing, water treatment, cosmetics, tissue engineering, etc.

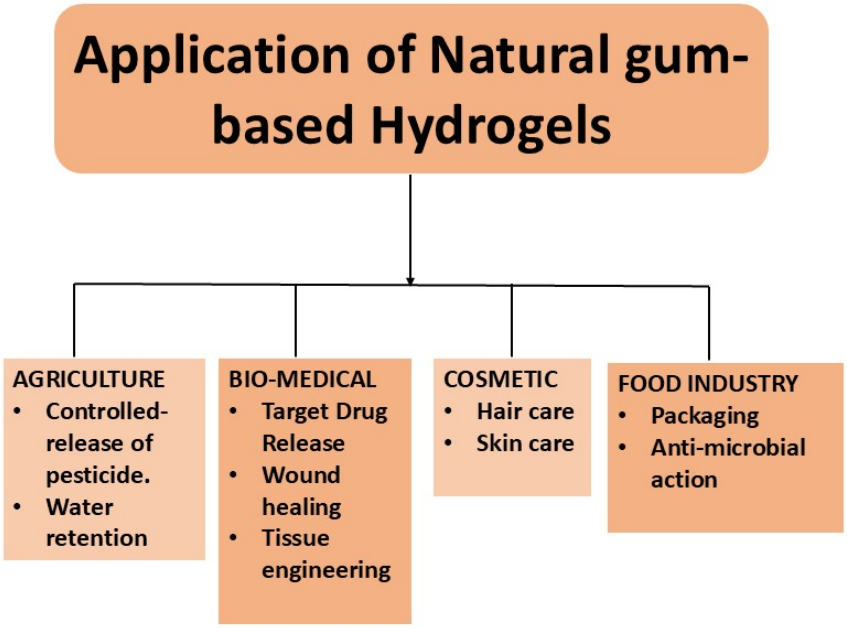

2.3.1 Agriculture

Hydrogels have wide applications in the agricultural sector due to their swelling and water-retention properties. Hydrogels provide a solution to water shortage problems. Hydrogels impact the water retaining and evaporation capacities of soil, and water flow from soil to roots for plant nutrition. Hydrogels are used as controlled-release devices of pesticides and fertilisers in plants, which reduces fertiliser loss and helps in plant growth [24].

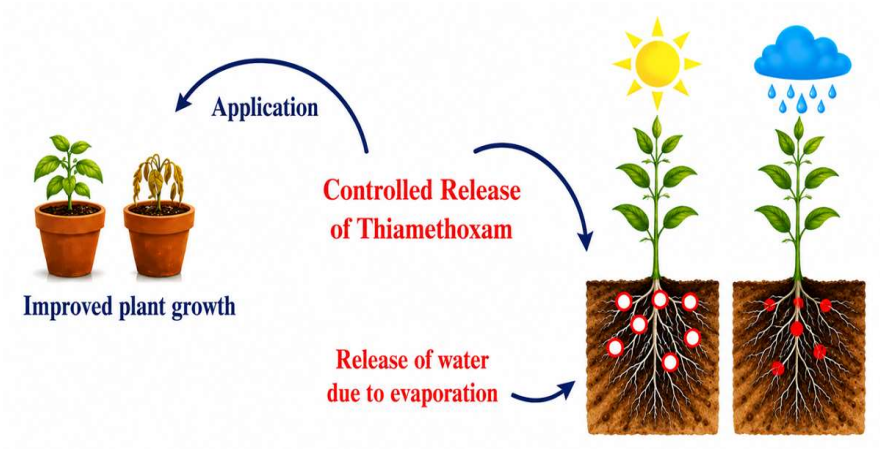

2.3.2 Food Industry

Hydrogel coatings and films have applications in the food industry, as natural gum-based hydrogels are biodegradable and non-toxic, it is used in food packaging. Hydrogel films maintain the atmosphere inside the food packaging and control the humidity by absorbing water caused by any temperature change or transpiration of fruits [25], [26].

2.3.3 Cosmetic

Hydrogels used in cosmetic preparations can be based on biopolymers, collagen, gelatine, alginate, chitosan, cellulose, and its derivatives. Biopolymer-based hydrogels are used to make innovative cosmetics such as beauty masks. These masks are supposed to hydrate skin, replenish its suppleness, and enhance anti-ageing efficacy. Superabsorbent hydrogels, particularly those composed of acrylate, are frequently used in hygiene products to absorb liquids because they prevent diaper rash, improve skin health, and provide comfort by keeping moisture away from the skin [27].

2.3.4 Bio-medical

As Hydrogel can mimic biological tissues, it can be used in biomedical application. Hydrogels are used in tissue engineering due to their swelling and deswelling, high compatibility, non-toxicity and high stability, as well as their degree of flexibility [28]. These properties are important for controlled target drug release. pH-sensitive hydrogels can show target drug delivery in the body at a specific pH [29].

CHAPTER 3: MATERIAL AND METHOD

3.1 Materials

Cassia fistula gum (CF) was procured from Hindustan Pvt. Ltd., Bhiwani, Haryana. *Acacia catechu* (ACT) was purchased from Vaibhav Trader, Bawana Industrial Area, New Delhi. Acrylic acid, sodium hydroxide (NaOH) and N′N-methylenebisacrylamide (MBA) were bought from CDH Pvt Ltd. Potassium persulphate (KPS) was bought from SD Fine Chem Ltd. Pesticide thiamethoxam was obtained from the Institute of Pesticide Formulation and Technology, Gurugram, India.

3.2 Methods

3.2.1 Synthesis of Hydrogels

Hydrogel was synthesised via free-radical copolymerization. A total of 16 formulations were synthesised (Table 2), in which KPS is used as an initiator, generating radicals for further polymerisation, while MBA was used as a crosslinker [30]. CF and ACT were dissolved in distilled water and stirred for 10-15 minutes to ensure proper dissolution. After that, a solution of polysodiumacrylate (PSA) was prepared by dissolving 4.2g NaOH in 10 mL of distilled water to obtain a homogeneous solution; then 7.2 mL of acrylic acid was added to the solution. PSA was added to the CFAC-g-SAH solution and stirred for 15-20 mins; then 0.1 gram of KPS was added and stirred continuously for 30-35 mins at room temperature. After 30 minutes, the crosslinker MBA was added, and the solution was stirred for another 30 minutes. Then the solution was transferred to a test tube and kept in a water bath for 30 minutes, maintaining the temperature around 60 °C [31], [32].

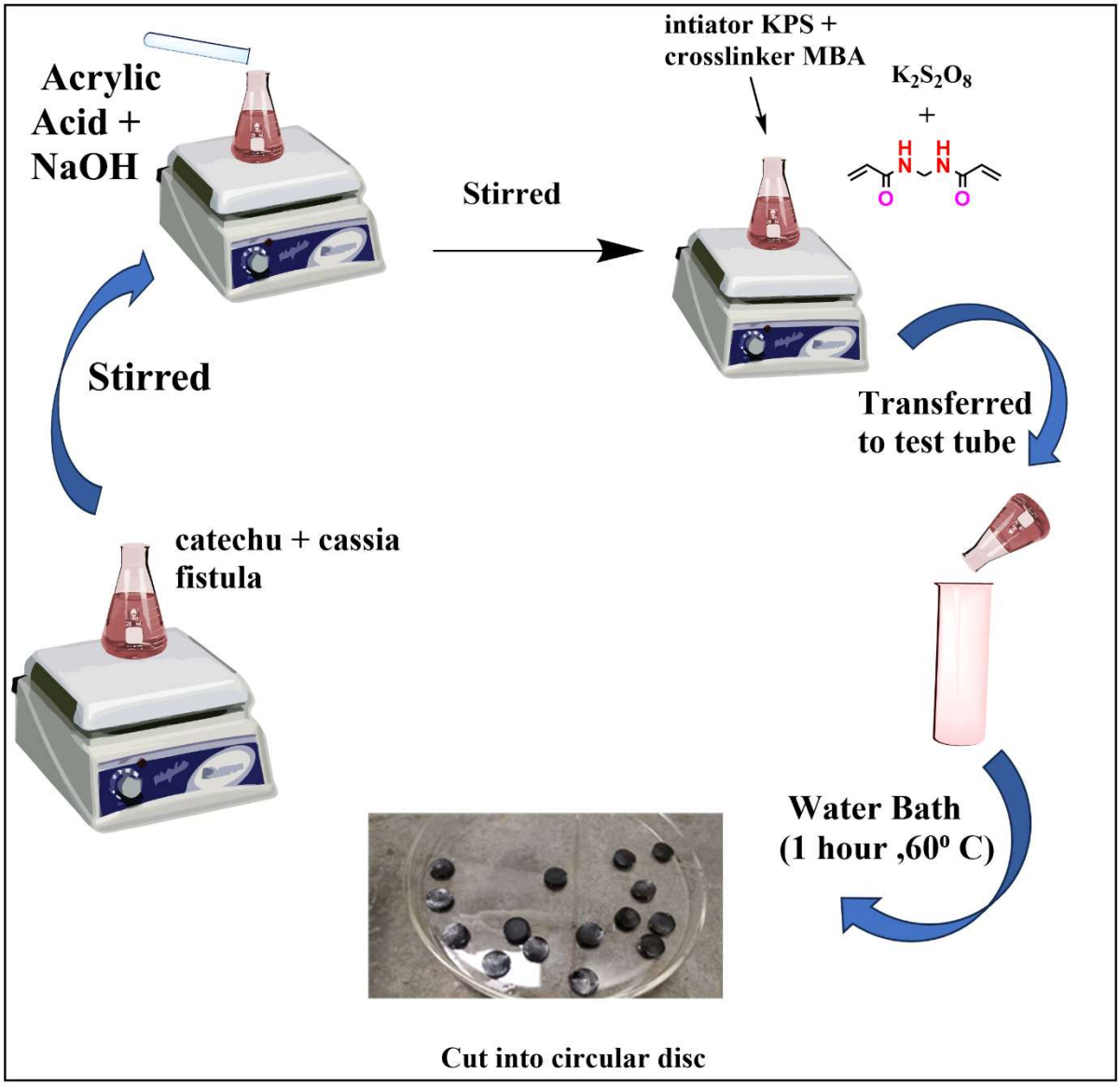

Figure 3.1 Pictorial illustration of the synthesis of a hydrogel

3.2.2 Swelling Studies

The swelling study of the Hydrogel was analysed using distilled water. A dry hydrogel pellet was weighed and immersed in distilled water [33]. The weight of the swollen hydrogel was measured at regular intervals of 1 hr at room temperature until equilibrium was achieved [34].

The extent of swelling of the hydrogel (swelling index) was investigated using equation 1 [17]:

$$Swelling\ index\ (g.g^{-1}) = \frac{m_2 - m_1}{m_1} \qquad (1)$$

Where m_1 and m_2 are the dry and swollen weights of the hydrogel, respectively.

3.2.3 Characterization

Solid state X-Ray Diffraction (PXRD) of samples CFAC, CF and ACT was examined for crystallography analysis using Panalytical's X'Pert Pro diffractometer with a range of 2θ from 10º to 2º/min and Cu Kα radiation. Solid-state ^{13}C CPMAS NMR analysis was conducted using a 400 MHz ECX-II JEOL spectrometer for structural characterisation. SEM was analysed using an EVO 18 Research instrument (Zeiss). FTIR, spectroscopic technique, used for analysing the functional groups of compounds and bonding modes in the Hydrogel using a Perkin-Elmer Model 2000 FTIR spectrometer, measuring between 4000 and 650 cm−1. The thermal stability of the synthesised hydrogel was also analysed by thermogravimetry analysis.

3.2.4 Loading and Release of Thiamethoxam

Fabricated Hydrogels were immersed in a 500 ppm thiamethoxam solution for 24 hours to achieve ex-situ loading. Then the thiamethoxam-loaded hydrogels were dried at 60 ºC. After the thiamethoxam-loaded hydrogels were completely dried, the release study was conducted in 100 mL of distilled water. At regular intervals, 3 mL of aliquots were drawn from the beaker using a micropipette, and an equal amount of distilled water was added to maintain a constant 100mL volume. The release study was observed for approximately 40 hours [35]. Pictorial representation of the controlled release mechanism of thiamethoxam is shown below in Figure 3.2. Loading percentage was calculated using an equation (2):

$$PL\ (\%) = \frac{A_L - A_R}{A_L} \times 100 \qquad (2)$$

Where A_L is the amount of thiamethoxam added to the hydrogel, and A_R is the amount of thiamethoxam remaining.

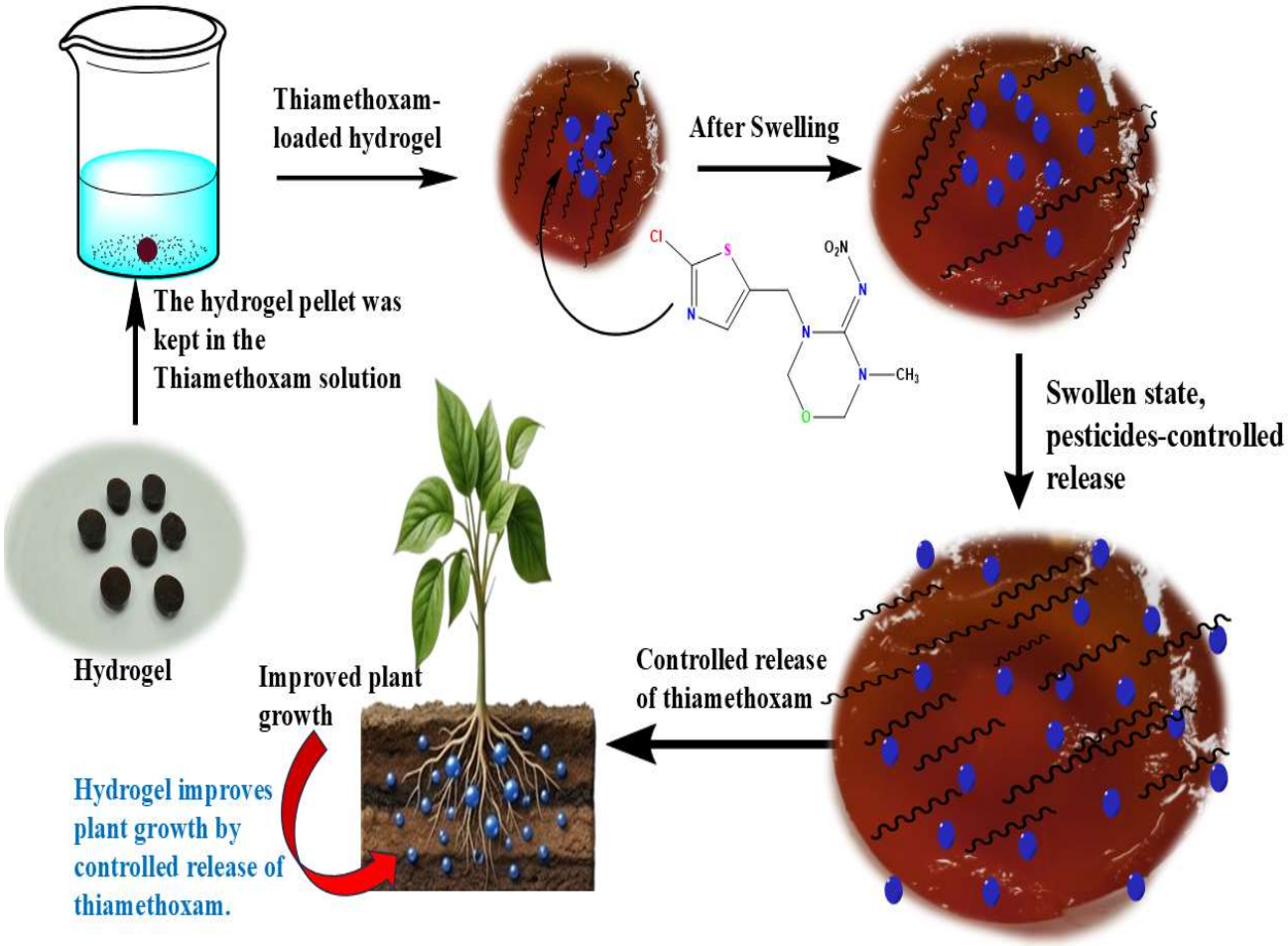

Figure 3.2 Pictorial illustration of the controlled release mechanism of Thiamethoxam

CHAPTER 4: Results and Discussion

4.1 Reaction Mechanism of Hydrogel

The fabricated hydrogels were synthesised through a free radical graft polymerization mechanism using KPS as initiator, as shown in Figure 4.1. Upon decomposition, KPS generated sulphate anions that take hydrogen atoms from the hydroxyl groups present in the backbone of CF and ACT. This results in the formation of macro radicals on the biopolymer chains. The active sites promote the growth of grafted poly (sodium acrylate) chains along the natural backbone. MBA formed covalent crosslinks between polymer chains, producing a three-dimensional network. The combination of polysaccharide CF and polyphenolic ACT components contributed to improving network architecture through hydrogen bonding and intermolecular interaction [36].

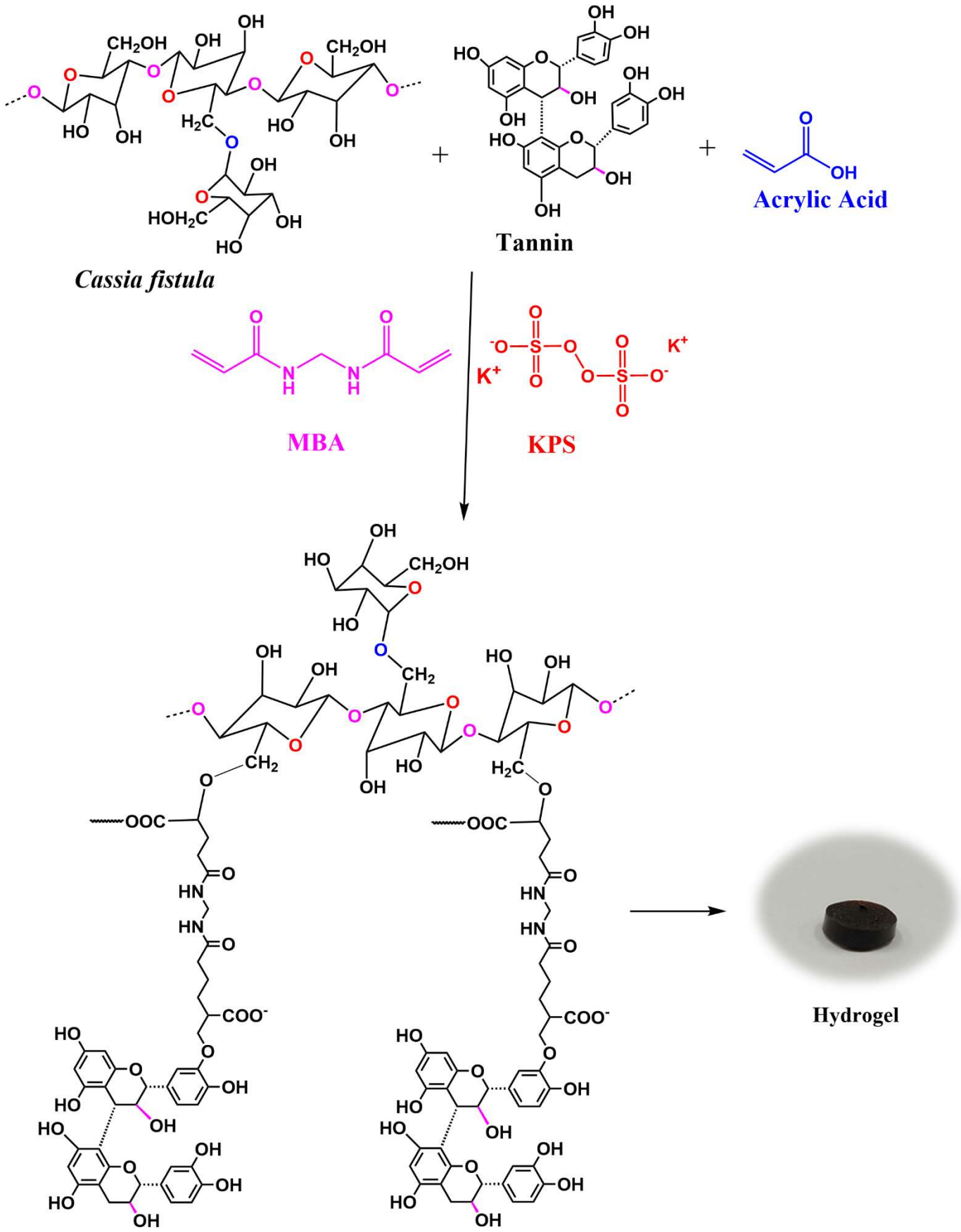

Figure 4.1 Schematic illustration of the possible Grafting mechanism of the synthesised Hydrogel.

4.2 Physical properties

After the water bath, hydrogels were cut into circular discs and oven-dried. The CFAC-g-SAH dry hydrogel pellet was a dark brown-coloured solid. This dry hydrogel pellet was kept in distilled water overnight; the swollen hydrogel was semi-solid and appeared orange-brown. The increased mass demonstrates substantial water uptake. Dry and swollen state images of CFAC-g-SAH, CF-g-SAH and ACT-g-SAH are shown in Figure 4.2(a-b), Figure 4.3 (a-b) and Figure 4.4(a-b), respectively.

Table 1 Physical appearance and properties of the synthesised hydrogels in dry and swollen state

Formulation	Before Swelling			After Swelling		
	Colour	Height(cm)	Diameter(cm)	Colour	Height(cm)	Diameter(cm)
CFAC-g-SAH	Dark Brown	0.4	1.3	Light Brown	1.7	4.6
ACT-g-SAH	Dark Brown	0.6	0.6	Brown	1.8	2.4
CF-g-SAH	Yellow	0.7	1.6	colourless	0.7	3

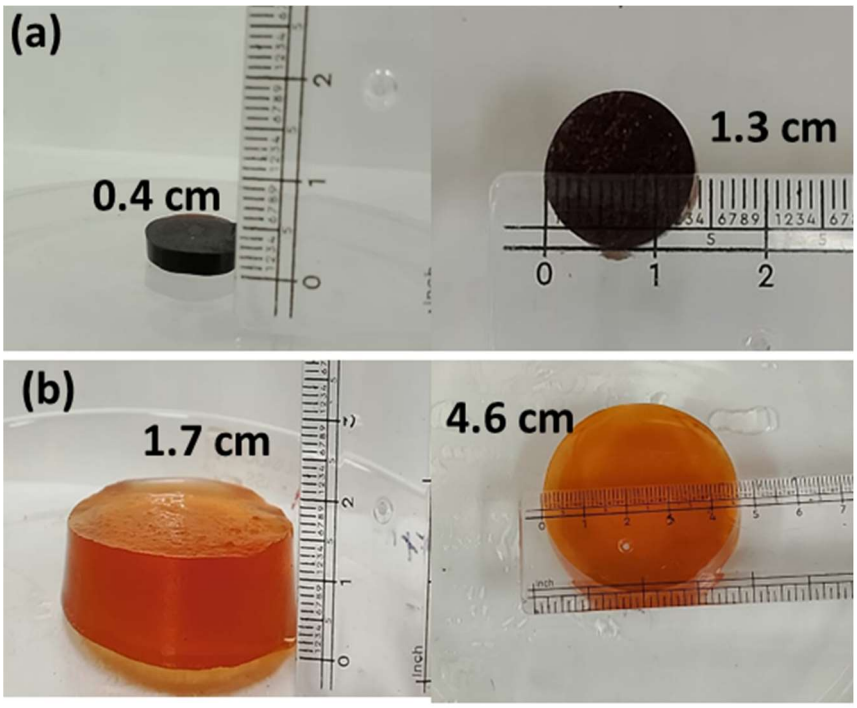

Figure 4.2 Picture of (a) before swelling and (b) after swelling of CFAC-g-SAH hydrogel

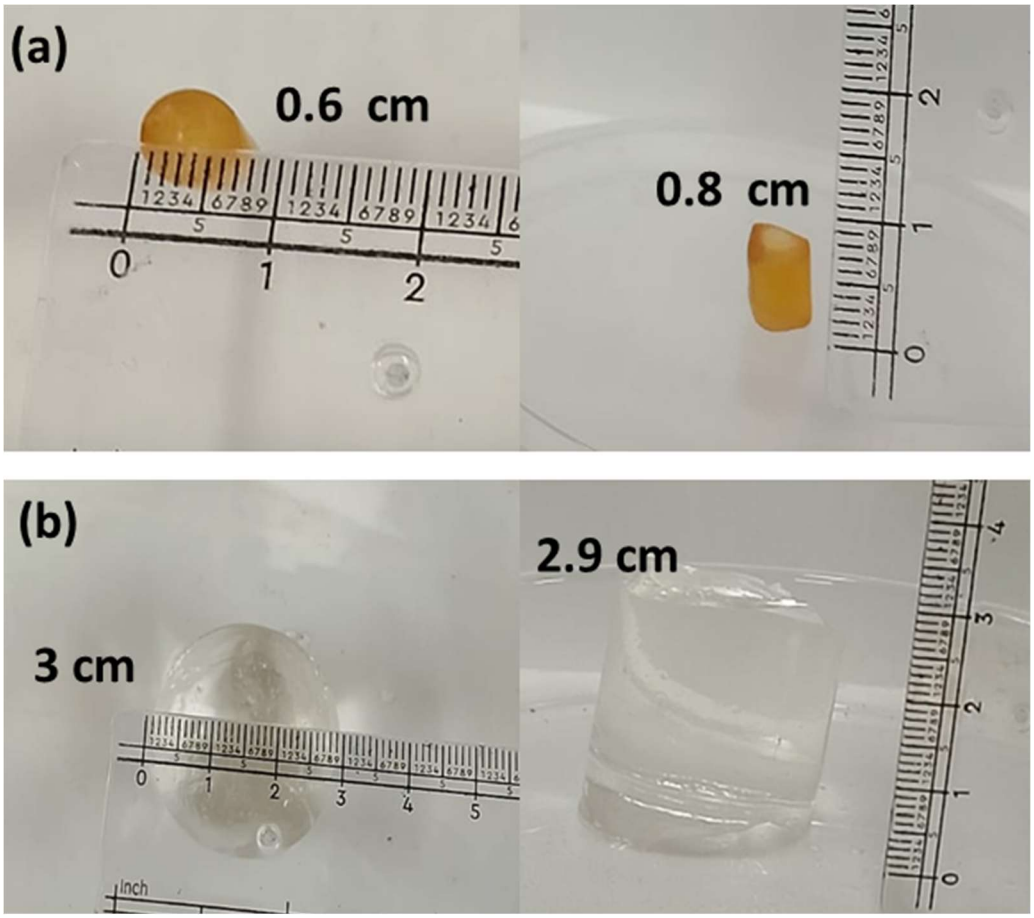

Figure 4.3 Picture of (a) before swelling and (b) after swelling of the CF-g-SAH hydrogel

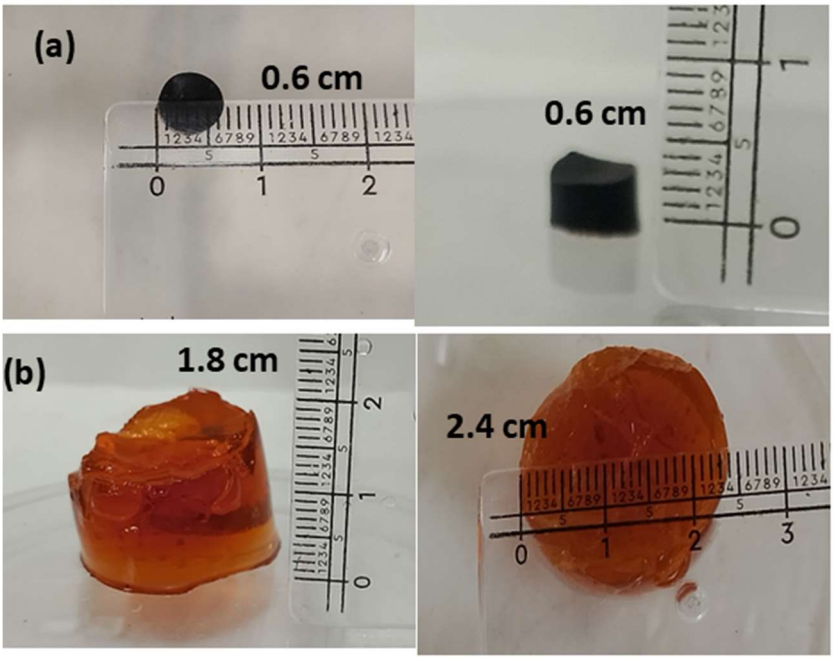

Figure 4.4 Picture of (a) Before Swelling and (b) After Swelling of ACT-g-SAH

4.3 Swelling study

Pellets of CFAC-g-SAH, CF-g-SAH and ACT-g-SAH were immersed in distilled water to study their swelling behaviour. The study reveals that CFCA-g-SAH had a swelling index of 185.94 ($g \cdot g^{-1}$) after 40 h, CF-g-SAH (125.05 $g \cdot g^{-1}$) after 37 h, and ACT-g-SAH (176.25 g·g-1) after 36 hr. From these swelling data, CFAC-g-SAH exhibited the greatest swelling among the synthesised hydrogels, as shown in Table 2. All three natural polymer-based hydrogels, i.e., CF-g-SAH, ACT-g-SAH, and CFAC-g-SAH, exhibited good swelling behaviour and can be used in drought-prone areas.

Table 2. Various formulations used in synthesis for the hydrogel, with their swelling index.

Formulation	CF (g)	ACT (g)	NaOH(g)	AA (mL)	MBA	KPS (g)	Swelling index ($g \cdot g^{-1}$)
CFAC-*g*-SAH 1	0.1	0.1	4.2	7.2	0.08	0.1	107.31
CFAC-*g*-SAH 2	0.2	0.1	4.2	7.2	0.10	0.1	109.85
CFAC-*g*-SAH 3	0.3	0.1	4.2	7.2	0.12	0.1	114.21
CFAC-*g*-SAH4	0.4	0.1	4.2	7.2	0.15	0.1	116
CFAC-*g*-SAH5	0.1	0.2	4.2	7.2	0.20	0.1	97.75
CFAC-*g*-SAH 6	0.2	0.2	4.2	7.2	0.08	0.1	185.94
CFAC-*g*-SAH7	0.3	0.2	4.2	7.2	0.14	0.1	85
CFAC-*g*-SAH8	0.4	0.2	4.2	7.2	0.12	0.1	117.94
CFAC-*g*-SAH9	0.1	0.3	4.2	7.2	0.12	0.1	88.04
CFAC-*g*-SAH 10	0.2	0.3	4.2	7.2	0.14	0.1	87.8
CFAC-*g*-SAH11	0.3	0.3	4.2	7.2	0.08	0.1	105
CFAC-g-SAH12	0.4	0.3	4.2	7.2	0.10	0.1	83.65
CFAC-g-SAH 13	0.1	0.4	4.2	7.2	0.14	0.1	108.54
CFAC-g-AA 14	0.2	0.4	4.2	7.2	0.12	0.1	137.09
CFAC-g-SAH15	0.3	0.4	4.2	7.2	0.10	0.1	178.77
CFAC-g-SAH16	0.4	0.4	4.2	7.2	0.08	0.1	117.66
CF-g-SAH	0.4	-	4.2	7.2	0.08	0.1	125.05
ACT-g-SAH	-	0.4	4.2	7.2	0.08	0.1	176.25

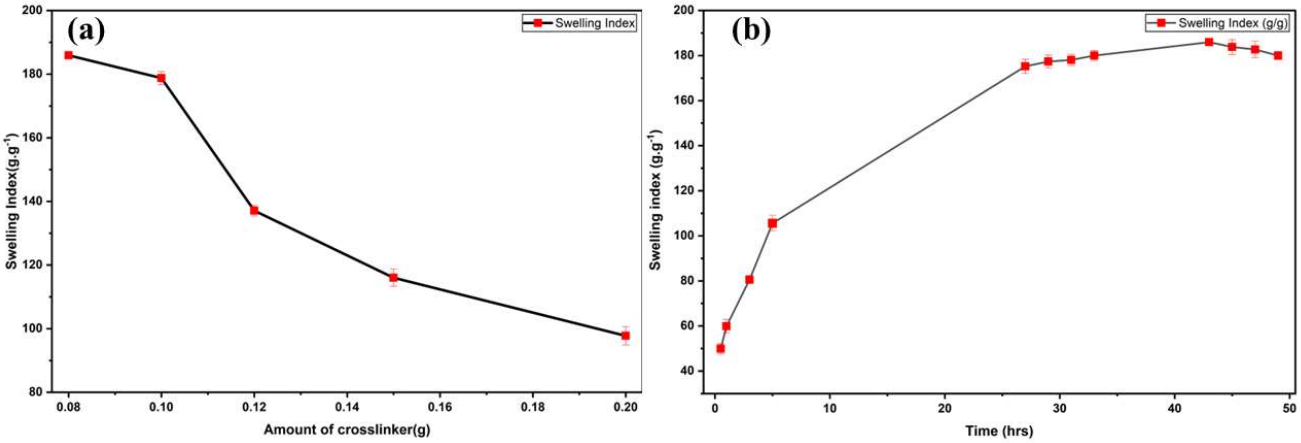

Figure 4.5 Variation of swelling index with (a) amount of crosslinker and (b) with time

4.3.1 Effect of Crosslinker on Swelling Index

As shown in Figure 4.5(a), SI ranged from 83 to 185.94 $g \cdot g^{-1}$ across formulations. Excessive crosslinking resulted in reduced swelling capacity. As MBA concentration increases, swelling index decreases systematically. MBA formed covalent links between grafted polyacrylate chains, which resulted in an increased crosslinking network between the polymeric chains. It reduces the porosity of the polymeric chain, thereby reducing its swelling capacity.

4.3.2 Variation in Swelling Index with Time

As shown in Figure 4.5(b), the swelling index increases with time, a property of hydrogels due to their hydrophilic nature. The swelling index increases until equilibrium is achieved, the hydrogel doesn't swell beyond the maximum water absorption, and the swelling index becomes nearly constant.

4.4. Characterization

4.4.1 ^{13}C-NMR

Figure 4.6 (a), (b), and (c) depicts the ^{13}C NMR spectrum obtained for ACT-*g*-SAH, CF-*g*-SAH and CFAC-*g*-SAH respectively. The peaks visible at 184.50 ppm, 181.70 ppm and 184.60 ppm correspond to the Carbon of carboxylate salt in all the synthesised hydrogels, which confirms graft polymerisation. Further peaks arise at 61.45 ppm, which is due to carbon of -CH_2OH of the galactose unit, and the carbon of the glycosidic linkage, and peaks at 60.73 ppm and 60.64 ppm are due to carbon attached to the hydroxyl group. Peaks visible at 39.528 ppm, 38.063 ppm and 38.453 ppm arise due to the aliphatic chains present in the hydrogel network [37], [38]. Another peak is visible at 110.942 ppm, 108.206 ppm, and 109.085 ppm, which are due to the presence of the pyranose cyclic ring of an anomeric carbon. As similar peaks are retained in the CFAC-*g*-SAH spectra, this confirms the affixing of CF with ACT [39].

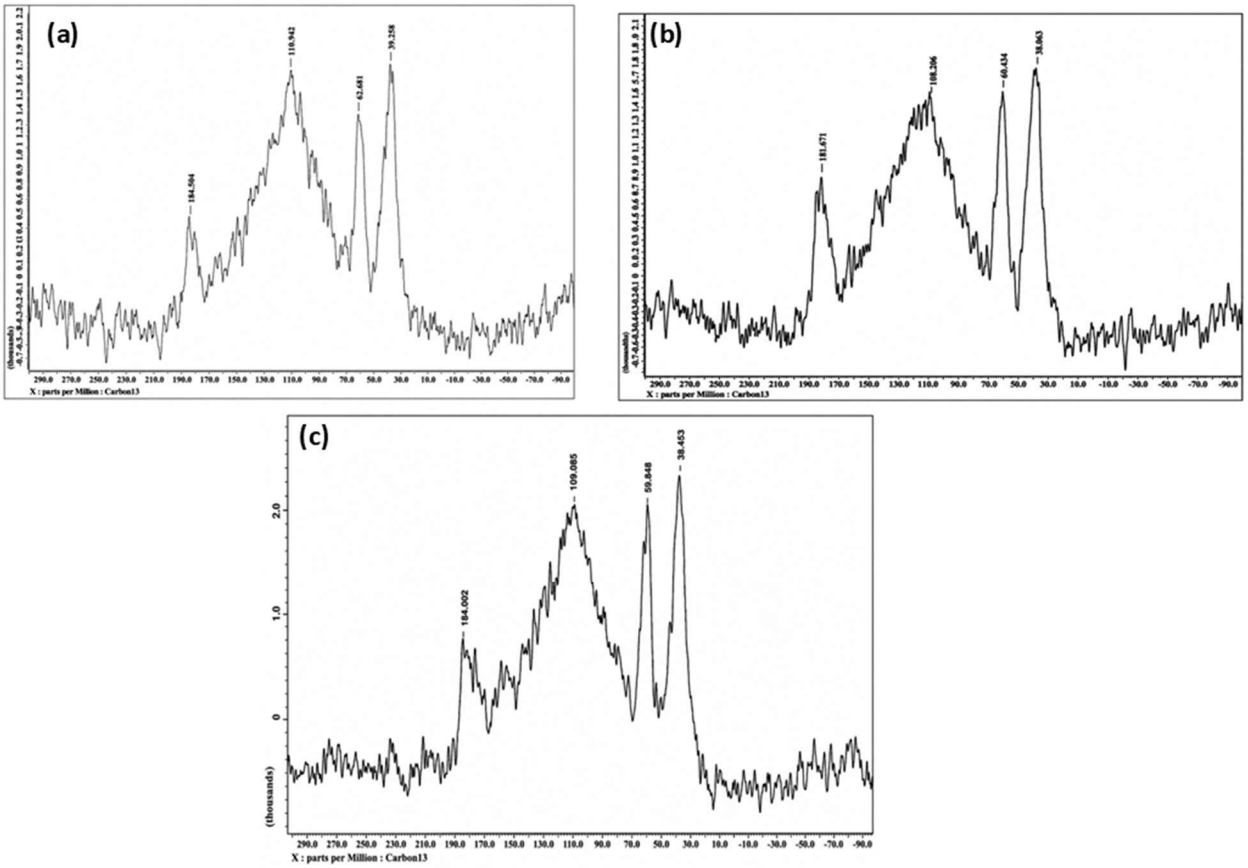

Figure 4.6 SS CPMASS ^{13}C NMR Spectra of (a) ACT-*g*-SAH, (b) CF-*g*-SAH and (c) CFAC-*g*-SAH

4.4.2 FT-IR

FTIR spectra of synthesised hydrogels CFAC-*g*-SAH, CF-*g*-SAH and ACT-*g*-SAH are shown below in Figure 4.7. All the hydrogels exhibit peaks ranging from 500 to 4000 cm^{-1}. All three hydrogels show broad peaks at 3033 cm-1, 3305 cm-1, and 3251 cm-1, respectively, indicating the presence of the O-H bond [31]. As ACT-*g*-SAH contains tannins, which are polyphenolic compounds, it shows a broader peak at a higher value [40][41]. Peaks 2934, 2949 and 2942 cm^{-1} indicate the presence of aliphatic C-H stretching. Peaks at 1716 and 1399 in CFAC-g-SAH, peaks at 1712 and 1404 cm^{-1} in CF-g-SAH and 1717 cm^{-1} and 1403 cm^{-1} in ACT-*g*-SAH indicate stretching vibrations for carbonyl of ─C═O and ─C─O found in the ─COONa group of the sodium acrylate. The sharp peaks 1557 and 1558 cm^{-1} might arise from the asymmetric vibrations of carboxylate ions. Peak at 88 for CF-*g*-SAH confirms the presence of anomeric deformation (α and β conformers) of pyranose, whereas the peak at 827 arises due to the presence of aromatic C-H [38].

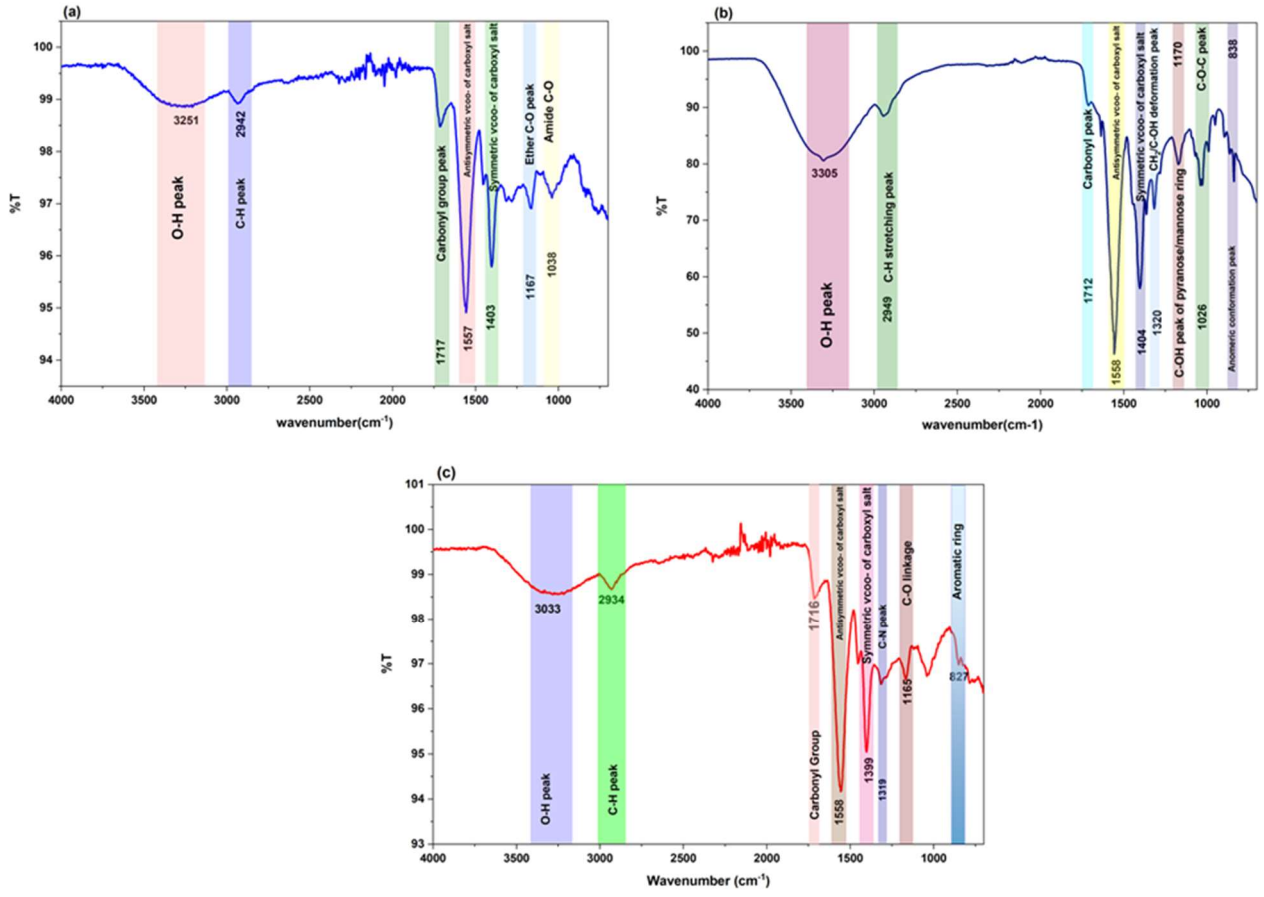

Figure 4.7 FTIR images of (a) ACT-*g*-SAH, (b) CF-*g*-SAH and (c) CFAC-*g*-SAH

4.4.3 SEM

The surface morphology of CF-*g*-SAH, CFAC-*g*-SAH, and ACT-*g*-SAH are shown below in Figure 4.8 at 1000x and 1500x magnification. It was observed that the hydrogel synthesised from combining the two biopolymers (CFAC-*g*-SAH) is highly porous compared to the control hydrogels (CF-*g*-SAH and ACT-*g*-SAH). This porous 3D network in hydrogels enabled water molecules to enter the matrix, resulting in greater swelling capability and improved release. CF-*g*-SAH images show a flat surface, mostly with very few pores, whereas ACT-*g*-SAH was slightly more porous than it, and the combination of both is highly porous in nature. Under external stimuli, the hydrophilic groups of polymers can interact with the porous structure of hydrogels. The heterogeneous porous morphology of hydrogel helps retain soil moisture for longer periods, supporting better crop production [42].

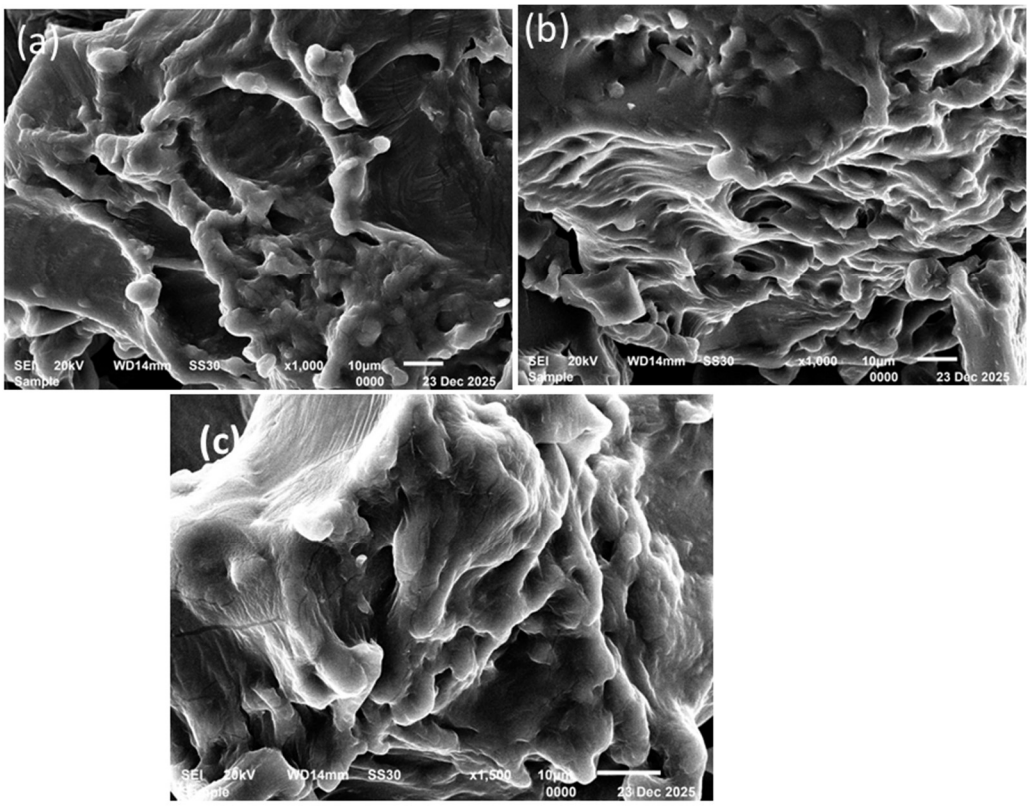

Figure 4.8 SEM images of (a) CF-*g*-SAH, (b) CFAC-*g*-SAH and (c) ACT-*g*-SAH

4.4.4 XRD

Powered XRD was performed for the synthesised hydrogels ACT-*g*-SAH, CF-*g*-SAH and CFAC-*g*-SAH. XRD patterns are shown below. Analysis was done in range of 10º-80º Bragg's angle(2θ) [43]. XRD spectra of CFAC-*g*-SAH, CF-*g*-SAH and ACT-*g*-SAH are shown in Figure 4.9. Only Broad peaks were observed nearly at 21.70º, 21.73º and 21.53º for CFAC-*g*-SAH, CF-*g*-SAH and ACT-*g*-SAH; all three broad peaks indicate that the samples are amorphous in nature [44]. Additionally, peaks observed at 31.86º, 31.88º and 32.01º for CF-*g*-SAH, ACT-*g*-SAH and CFAC-*g*-SAH respectively, are due to the grafting process. The amorphous nature of hydrogel is advantageous for swelling and controlled release, as reduced crystallinity enhances water penetration and diffusion of encapsulated pesticide.

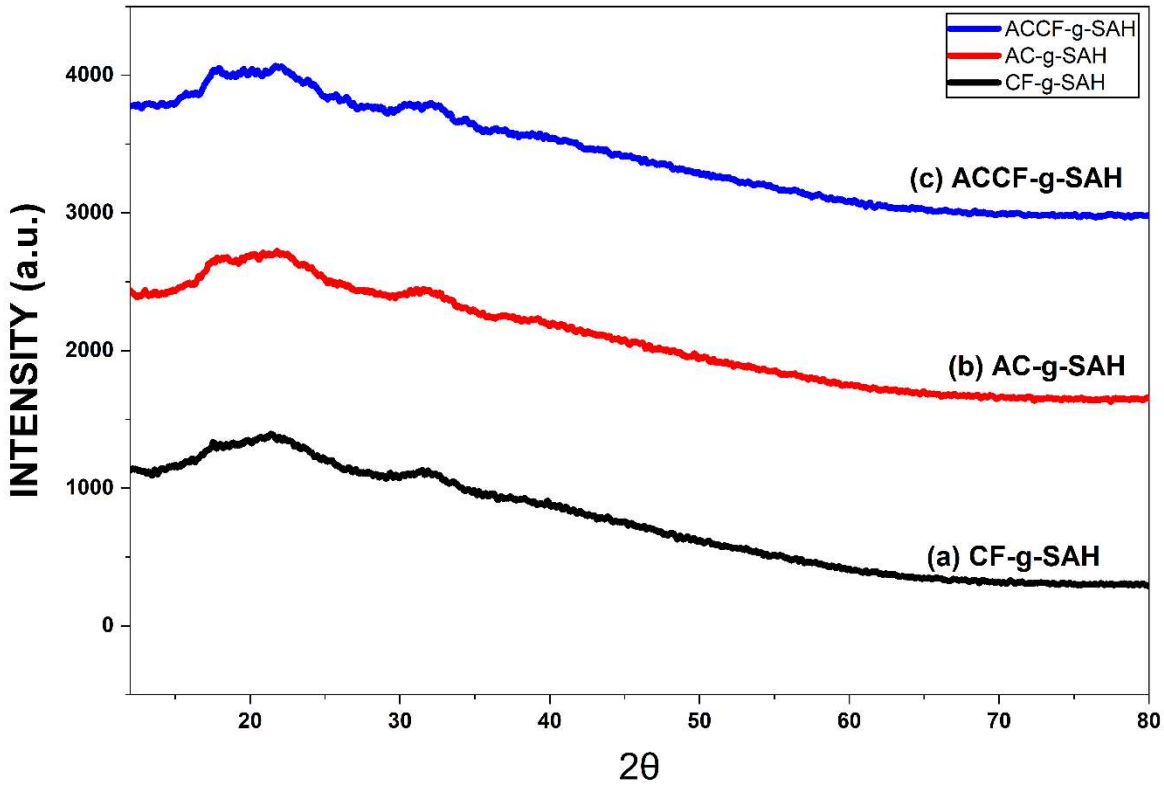

Figure 4.9 XRD Plot for CFAC-*g*-SAH, ACT-*g*-SAH and CF-*g*-SAH

4.4.5 TGA

The Thermal stability of hydrogels is determined by using the thermogravimetric analysis (TGA). The spectra of CFAC-*g*-SAH, ACT-*g*-SAH and CF-*g*-SAH are shown in Figure 4.10. This spectrum shows a degradation pattern in four steps between the ranges 28-600 ºC. The first degradation between the ranges of 29.72 ºC -138.96ºC, 29.97ºC – 126.51ºC and 30.43ºC-106.95ºC with mass loss at 5.72 %, 2.5 % and 3.3 % in CFAC-*g*-SAH, ACT-*g*-SAH and CF-*g*-

SAH, respectively, is due to the volatilisation of smaller compounds with low molecular weight and the evaporation of water molecules. Second degradation step ranges between 138.96 ºC-351.53 ºC, 126.51ºC- 255.2 ºC and 106.95ºC-247.53 ºC for all synthesised hydrogels, indicating the degradation of the polysaccharide backbone and small ungrafted molecular polymer of ACT and CF, with mass degraded as 12.19%, 6.95% and 7.77% for CFAC-*g*-SAH, ACT-*g*-SAH and CF-*g*-SAH respectively, [45], [46]. The third step depicts bond breakage of polymeric backbone in the range of 351.53ºC- 430ºC, 255.2 ºC - 407.56ºC and 247ºC- 422 ºC for CFAC-*g*-SAH, ACT-*g*-SAH and CF-*g*-SAH respectively, with a weight loss of 15.06%, 10.79% and 11.57% for CFAC-*g*-SAH, ACT-*g*-SAH and CF-*g*-SAH respectively. The final degradation step was observed up to 591ºC, depicting degradation of strongly bonded entities. The remaining residues for CFAC-*g*-SAH, ACT-*g*-SAH and CF-*g*-SAH are 47.2%, 48.43% and 47.2% [47].

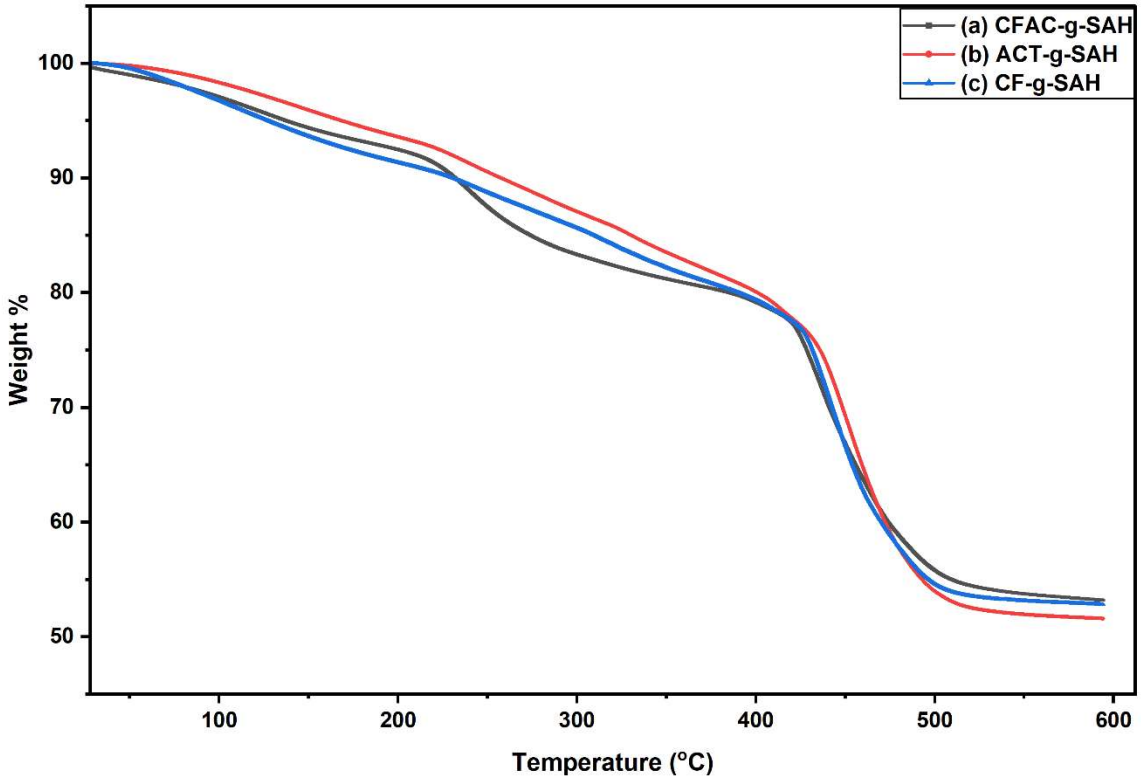

Figure 4.10 TGA spectra of (a) CFAC-*g*-SAH, (b) ACT-*g*-SAH and (c) CF-*g*-SAH

4.5. Release Study

The release study of thiamethoxam encapsulated in the synthesised hydrogels CFAC-g-SAH, ACT-*g*-SAH, and CF-*g*-SAH was conducted in distilled water for 38-40 hours. The loading percentage of thiamethoxam in the CFAC-*g*-SAH, CF-*g*-SAH, and ACT-*g*-SAH was 58.49%, 36.39%, and 42.43%, respectively. Kinetic models used to examine release kinetics included the Korsmeyer-Peppas, Higuchi, and first-order models. The higher loading capacity of CFAC-*g*-SAH is attributed to its higher swelling index and porous morphology, which provides greater free volume and active sites for pesticide entrapment.

The Korsmeyer-Peppas model describes the pesticide release with the help of the release exponent. In cylindrical systems, exponent values between 0 and 0.45 show Fickian diffusion, and values in the range of 0.45 to 0.89 describe anomalous transport. Also, for the KP model, the release pattern must be less than 60% [48]. Fickian diffusion indicates that the pesticide has been released through the matrix by diffusion, whereas non-Fickian diffusion indicates that the pesticide has been released as a result of diffusion and relaxation of the carrier matrix [31], [49].Power law equation used for the KP model equation 3:

$$\frac{M_t}{M_\infty} = K_{kp}.t^n \qquad (3)$$

Where M_t and M_∞ represent thiamethoxam releases at time t and the equilibrium point, respectively.

The value of n characterises the release mechanism. Figure 4.11 (a), (b) and (c) depict the release kinetics of CFAC-*g*-SAH, CF-*g*-SAH and ACT-*g*-SAH.

The Higuchi model explains that pesticide release takes place via diffusion only. This model studies the release in terms of the square root of time, shown in Figure 4.13 (a), (b) and (c) for CFAC-*g*-SAH, CF-*g*-SAH and ACT-*g*-SAH. First-order kinetics explains that the rate is proportional to the remaining amount of pesticide in the hydrogel matrix [50]. First order kinetics is depicted in Figure 4.14 (a), (b) and (c). Table 3 shows that the value of n is 0.69, 0.57, and 0.60 for CFAC, CF, and ACT hydrogels, respectively, indicating that the release of thiamethoxam proceeds via a non-Fickian mechanism. The value of the regression coefficient $R^2 = 0.99$ confirms the validation of the Korsmeyer-Peppas model and first-order mechanism for CFAC-*g*-SAH and ACT-*g*-SAH. Whereas CF-g-SAH follows the Korsmeyer-Peppas and Higuchi models for diffusion [51], [52]. The results demonstrate that CFAC-*g*-SAH functions

as an efficient controlled-release carrier, capable of reducing pesticide loss through leaching and enhancing utilisation efficiency.

Table 3: Kinetic Models for the release kinetics of thiamethoxam.

Model	Equation	Parameter	Values		
			CFAC-g-SAH	CF-g-SAH	ACT-g-SAH
Korsmeyer Peppas	$f = k_{kp} \cdot t^n$ k_{kp} = rate constant f = amount of the release pesticide	K_0 (min^{-1}) R^2 n	10.926 0.99 0.69	11.19 0.99 0.57	4.890 0.99 0.60
Higuchi	$f = k_H t^{0.5}$ f = amount of released pesticide t = time k_H = Higuchi dissolution constant	K_H ($min^{-0.5}$) R^2	8.857 0.81	13.77 0.98	13.03 0.89
First order	$f = 100[1-e^{-kt}]$ f = amount of released pesticide k = rate constant t = time	K_1 (min^{-1}) R^2	0.083 0.98	0.073 0.88	0.042 0.98

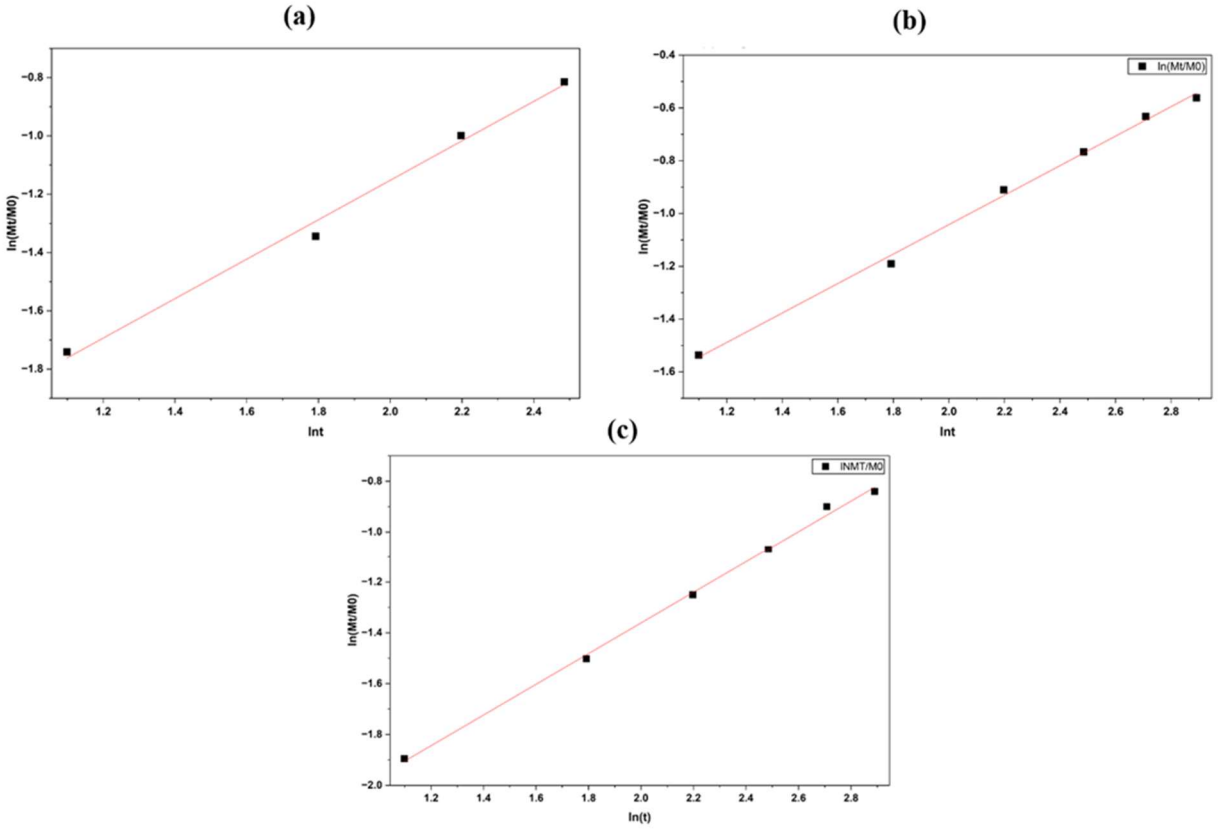

Figure 4.11 Release kinetics of KP model for (a) CFAC-*g*-SAH, (b) CF-*g*-SAH and (c) ACT-*g*-SAH.

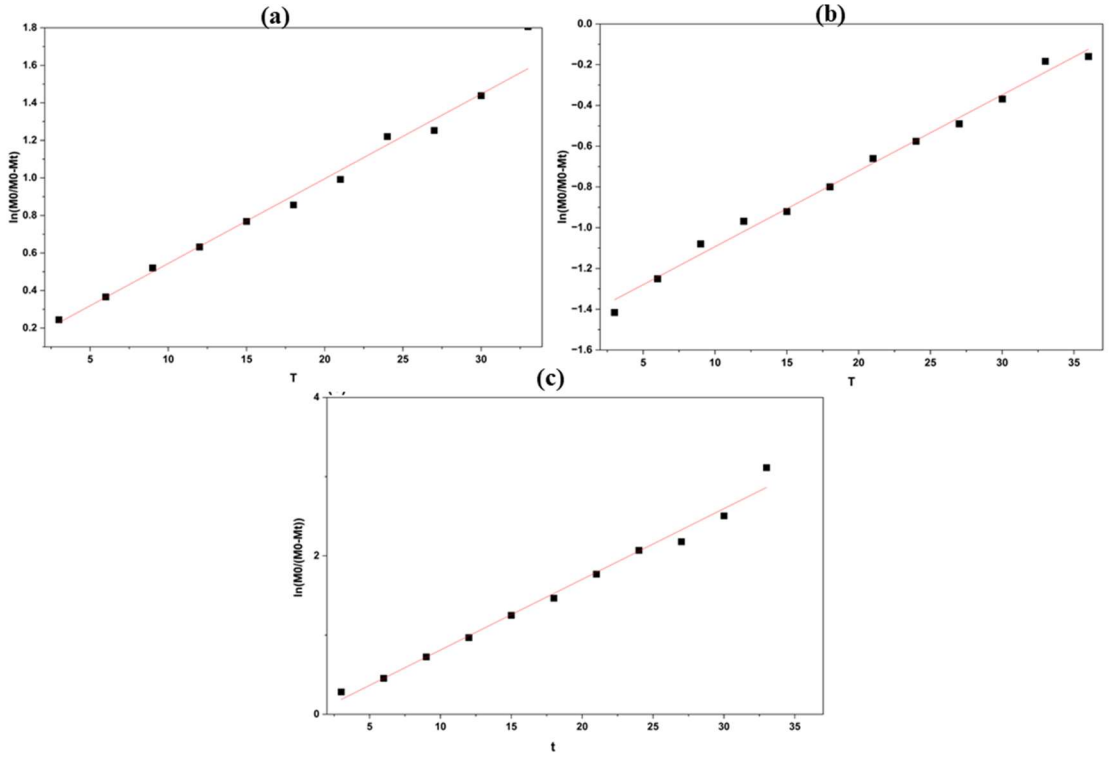

Figure 4.12 Release kinetics of First order for (a) CFAC-*g*-SAH, (b) CF-*g*-SAH and (c) ACT-*g*-SAH.

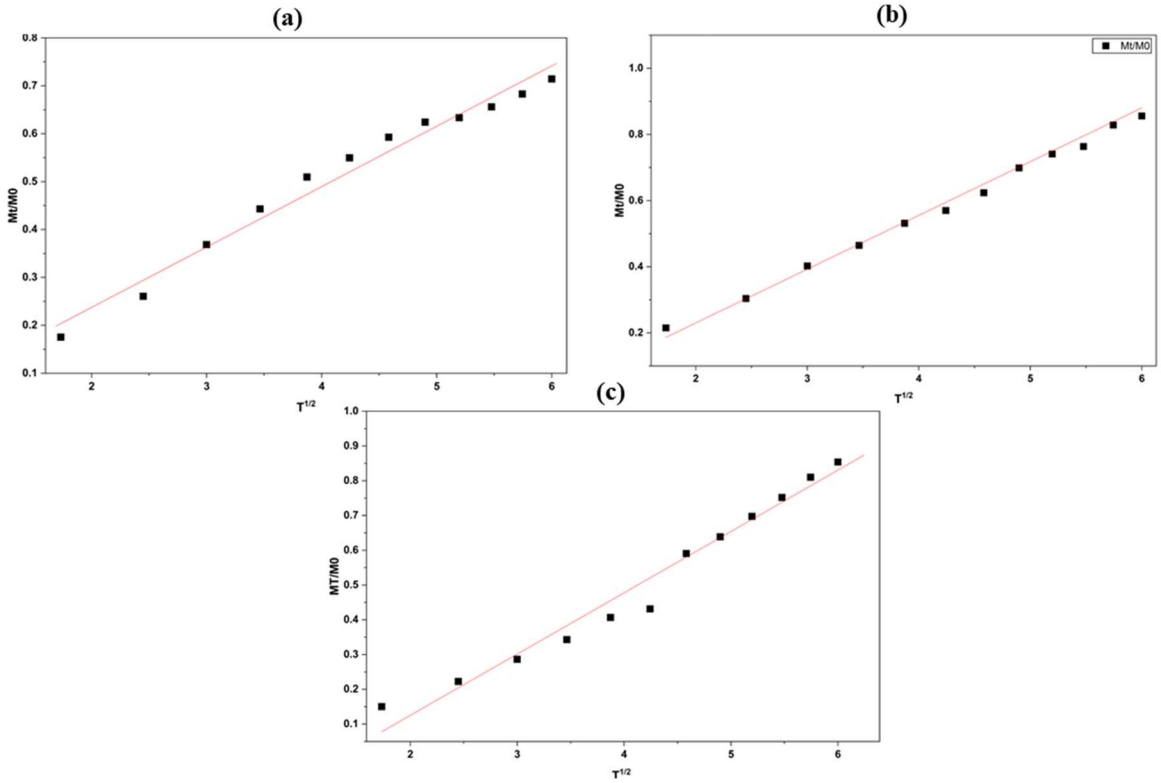

Figure 4.13 Release kinetics of the Higuchi model for (a) CFAC-*g*-SAH, (b) CF-*g*-SAH and (c) ACT-*g*-SAH.

CHAPTER 5: CONCLUSION

A novel grafted hydrogel incorporating tannin from *Acacia catechu* and *Cassia fistula* was successfully synthesised via free radical copolymerization for controlled thiamethoxam delivery. The synthesised hydrogels were characterised using FT-IR and NMR spectroscopy to determine functional groups and chemical structure. Surface morphology was characterised using SEM and XRD. The thermal stabilities of the synthesised hydrogel were examined using TGA. The optimised formulation (CFAC-*g*-SAH6) exhibited the highest swelling capacity (185.84 g/g), enhanced porosity, and the highest pesticide loading efficiency compared to ACT-*g*-SAH and CF-g-SAH. The loading percentages of thiamethoxam were 58.49%, 36.39%, and 42.43% for CFAC-g-SAH, CF-g-SAH, and ACT-g-SAH, respectively. The CFAC-g-SAH hydrogel outperformed ACT-g-SAH and CF-g-SAH in terms of the highest swelling and longest release duration. Sustained release over approximately 40 h, governed by non-Fickian diffusion behaviour, confirms the hydrogel's ability to regulate pesticide transport through combined diffusion and matrix relaxation mechanisms. The synergistic interaction between polysaccharides and polyphenols resulted in improved network architecture, enhanced water uptake, and controlled diffusion properties. Overall, CFAC-*g*-SAH demonstrates strong potential as an eco-friendly, sustainable controlled-release system for agricultural applications. Its ability to enhance pesticide efficiency while reducing environmental contamination makes it a promising candidate for advanced agrochemical delivery platforms.

JOURNAL OF MACROMOLECULAR SCIENCE, PART B
https://doi.org/10.1080/00222348.2026.2686685

Taylor & Francis
by Informa

Check for updates

Crosslinking of Tannin and *Cassia fistula* Gum Engenders a Smart Hydrogel for Controlled Release of Thiamethoxam

Mamata Singh, Vaishali Prashar, Manu Nandal, Devendra Kumar, and Rajinder K. Gupta

Department of Applied Chemistry, Delhi Technological University, New Delhi, India

ABSTRACT

In this study, *Cassia fistula* (CF) gum and Tannin from *Acacia catechu* (ACT), potentially used to produce CFAC-g-SAH for effective controlled-release of agrochemicals. The synthesized hydrogels were thoroughly characterized by ^{13}C NMR, FT-IR, SEM, XRD, and TGA. CFAC-g-SAH was compared with ACT and CF hydrogels. The swelling studies of the synthesized hydrogel were measured by varying amounts of crosslinker and biopolymer, yielding the highest swelling for CFAC-g-SAH 185 g g^{-1}. Release kinetics of synthesized hydrogels were studied by the Korsmeyer–Peppas, Higuchi and first-order kinetics models. The loading percentages of thiamethoxam were 58.49, 36.39, and 42.43% for CFAC-g-SAH, CF-g-SAH, and ACT-g-SAH, respectively. The CFAC-g-SAH hydrogel outperformed ACT-g-SAH and CF-g-SAH in highest swelling and longest release duration. A sustained release up to 40 h was achieved using CFAC-g-SAH, followed by a non-Fickian release mechanism. Thus, the synthesized CFAC-g-SAH emerges as a promising controlled-release device for agrochemicals with the potential to mitigate the environmental impact of pesticides.

ARTICLE HISTORY
Received 2 April 2026
Accepted 2 June 2026

KEYWORDS
Cassia fistula; controlled release; hydrogel; Tannin; thiamethoxam

GRAPHICAL ABSTRACT

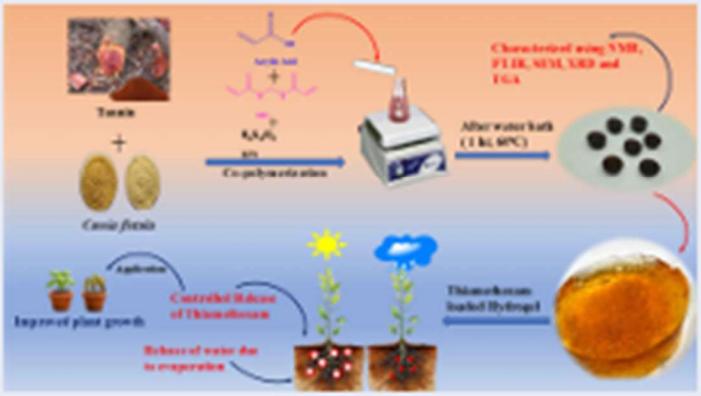

CONTACT Rajinder K. Gupta rkg67ap@yahoo.com; dkumar@dce.ac.in Department of Applied Chemistry, Delhi Technological University, Bawana Road, Shahbad Daulatpur village, New Delhi 110042, India

Supplemental data for this article can be accessed online at https://doi.org/10.1080/00222348.2026.2686685.